# Novel targets in the liver to treat cardiometabolic diseases

Ge, X.

# CHAPTER 4

## A rare gain of function variant of hepatic lipase attenuates hypercholesterolemia and atherosclerosis in mice via an LDL receptor-independent mechanism

Thibaud Sotin*, Xiaoke Ge*, Milena Schönke, Lucie Vince, Amélie Thouzeau, Samuel Frey, Victoria Lorant, Lisa Krul, Amanda C.M. Pronk, Reshma Lalai, Trea C.M. Streefland, Salwa Afkir, Wieneke Dijk, Sarra Smati, Marieke Heijink, Niek Blomberg, Martin Giera, Mathilde Di Filippo, Philippe Moulin, Sander Kooijman, Bertrand Cariou#, Patrick C.N. Rensen#, Cédric Le May#

***Co-first author; #Co-senior author**

**Cardiovasc Res 2025, 121: 1024–1035**

## Abstract

**Aims**: *LIPC* encodes hepatic lipase (HL), a liver-bound protein with both phospholipase and triglyceride lipase activity, and involved in the catabolism of circulating lipoproteins. We recently identified the gain-of-function variant HL-E97G, with selectively increased phospholipase activity, as a new genetic cause of familial combined hypocholesterolemia in humans. The role of HL in the development of atherosclerosis remains controversial. In this context, the action of HL-E97G on the development of atherosclerosis remains unknown.

**Methods and Results**: To evaluate the lipid-lowering and anti-atherogenic properties of HL-E97G versus wild-type HL (HL-WT) in hypercholesterolemic *APOE*3-Leiden.CETP* mice, a well-established model for human-like lipoprotein metabolism, and to assess dependence of these effects on the LDL receptor (LDLR) pathway in LDLR-deficient (*Ldlr*$^{-/-}$) mice. *APOE*3.Leiden.CETP* mice or *Ldlr*$^{-/-}$ mice received an intravenous injection of AAV8 expressing either eGFP (control), HL-WT or HL-E97G ($3\times10^{11}$ GC/mouse) while being fed pro-atherogenic diets. Plasma cholesterol levels were measured monthly, and aortic atherosclerotic lesion sizes were assessed at termination. HL-E97G largely decreased plasma total cholesterol exposure in APOE*3-Leiden.CETP mice (-63% vs control; -58% vs HL-WT), resulting at least in part from increased uptake of (V)LDL by the liver, accompanied by a marked decrease in atherosclerotic lesion size (-98% vs control; -97% vs HL-WT) in the aortic root. Importantly, HL-E97G also strongly reduced plasma cholesterol exposure in *Ldlr*$^{-/-}$ mice (-80% vs control; -77% vs HL-WT), and decreased atherosclerotic lesion size in the aortic root (-54% vs control; -41% vs HL-WT) and the aortic arch (-73% vs control; -70% vs HL-WT).

**Conclusions:** HL-E97G strongly reduces plasma cholesterol levels, by increasing the uptake of (V)LDL, to decrease atherosclerosis development in mice independently of the LDLR pathway. These data suggest that modulating HL function is a promising tool in patients with familial hypercholesterolemia.

## Introduction

Atherosclerotic cardiovascular disease (ASCVD) is the leading cause of premature death worldwide, accounting for as many as 20 million deaths annually.[1,2] Dyslipidemia, particularly elevated low-density lipoprotein cholesterol (LDL-C) concentration, remains one of the most important modifiable risk factors for ASCVD.[3] Exposure to lower cumulative concentrations of LDL-C in young or middle-aged individuals is associated with a reduction in long-term ASCVD risk.[4] In addition, the results of cardiovascular outcomes randomized trials with powerful lipid-lowering therapies (LLTs), such as proprotein convertase subtilisin/kexin type 9 (PCSK9) inhibitors, have led to a progressive lowering of the LDL-C target for the prevention of ASCVD in international guidelines, reaching 55 mg/dL (1.4 mM) for patients at highest risk.[5] However, a significant proportion of individuals, especially those at very high risk of ASCVD, do not achieve LDL-C targets due to treatment intolerance, low compliance, or ineffectiveness despite the emergence of numerous innovative therapeutic solutions in recent years.[6,7]



In this context, a particular clinical situation is that of homozygous familial hypercholesterolemia (HoFH), a rare disease characterised by very high concentrations of LDL-C and premature atherosclerosis occurring from childhood onwards in the absence of management.[8] Since patients with HoFH can have no residual LDL receptor (LDLR) function according to the severity of mutation, the standard LLTs (i.e. statins and PCSK9 inhibitors) are either ineffective or only marginally effective because their mode of action is through upregulation and stabilization of the LDLR.[9,10] Recently, a randomized controlled trial demonstrated that evinacumab, an inhibitor of angiopoietin-like 3 protein (ANGPTL3) was safe and effective in all HoFH subgroups.[8,11] Lomitapide, an inhibitor of microsomal triglyceride transfer protein, was also reported to reduce LDL-C levels in HoFH, but issues with adverse events (i.e. liver steatosis), tolerability with gastrointestinal disturbances, and adherence were identified.[10] Finally, in these HoFH patients, weekly or twice-weekly LDL-apheresis remains an essential therapeutic strategy.

Interestingly, we recently identified a novel rare variant in the *LIPC* gene (HL-E97G) in a large pedigree of individuals with both low LDL-C and high-density lipoprotein cholesterol (HDL-C) concentrations as a genetic cause of familial combined hypolipidemia.[12] *LIPC* encodes hepatic lipase (HL), which belongs to the family of glycerol-sn-1 fatty acid hydrolases that includes lipoprotein lipase (LPL) and endothelial lipase (EL).[12] HL has a balanced hydrolytic activity for both triglycerides (TG) and phospholipids (PL),[12,13] and plays an important role in lipoprotein metabolism by catabolizing HDL-C and TG-rich lipoproteins (reviewed in [13]). We showed that HL-E97G is a gain-of-function variant of HL with selectively increased phospholipase activity.[12] Hepatic expression of HL-E97G in male *APOE*3.Leiden.CETP* mice

reduces plasma PL, TG and cholesterol levels compared to HL-WT, mimicking the combined hypolipidemia observed in individuals who carry the HL-E97G variant.[12]

Given that the proband in the family had revascularized coronary artery disease[12] and the significant drop in HDL-C, it was important to determine the impact of the HL-E97G variant on the development of atherosclerosis. Here, we investigated the effect of hepatic expression of HL-E97G versus HL-WT on atherosclerosis development in hypercholesterolemic *APOE*3.Leiden.CETP* mice, a well-established model of human lipoprotein metabolism, and also in LDLR-deficient (*Ldlr*$^{-/-}$) mice in order to determine the importance of the LDLR pathway in the effects of the HL-E97G variant.

## Methods



### Mouse studies

*APOE*3-Leiden.CETP* mice (C57Bl/6J background) were bred at Leiden University Medical Center (Leiden, the Netherlands), and used for experiments as approved by the Animal Welfare Body Leiden and executed under a license granted by the Central Authority for Scientific Procedures on Animals (CCD) under the license number AVD11600202010187 in accordance with the Dutch Act on Animal Experimentation and EU Directive 2010/63/EU. *Ldlr*$^{-/-}$ mice (C57Bl/6J background) were bred at Nantes Université animal facility (Nantes, France), and used for experiments as approved by the ethics committee of Pays de la Loire (France, 006) and the Ministère de l'Enseignement supérieur et de la Recherche (France; APAFIS 26862). All mice were group housed under a 12-hour light-dark cycle, at 22°C, and had free access to water and food unless indicated otherwise.

In a first experiment, *APOE*3.Leiden.CETP* mice (8-14 weeks old) were fed a Western-type diet (Ssniff Spezialdiäten GmbH, Germany) containing 16% fat and 0.15% cholesterol. We used females only as males fail to increase circulating cholesterol on a Western-type diet and develop only very small lesions.[14] Following a 3-week dietary run-in period to induce hyperlipidemia, mice were assigned to blocks (n = 16 per group) that were balanced for plasma total cholesterol (TC), TG, PL and body weight using RandoMice.[15] Groups were randomly assigned to receive an intravenous injection with $3\times10^{11}$ genome copies of adeno-associated viruses (AAV8) expressing, under the thyroxin-binding globulin (TBG) promoter, either enhanced green fluorescent protein (eGFP; control), the human *LIPC* gene encoding wildtype HL (HL-WT), or the human *LIPC* gene encoding the gain-of-function E97G variant of HL (HL-E97G) (Vector Biolabs, USA).

In a second experiment, male and female *Ldlr*$^{-/-}$ mice (10-14 weeks old) were block-randomized into three groups (n = 8-10 per group) balanced for plasma TC, TG and body

weight using RandoMice,[15] and fed with a pro-atherogenic diet containing 17% cocoa butter, 1.25% cholesterol and 0.5% cholic acid (Research Diet #D12109Ci, USA). Upon switching to this diet, mice received intravenous injections of the same viruses at the same dose as the *APOE*3-Leiden.CETP* mice.

**Body weight, organ weight and blood biochemistry**

Mice were weighed on a weighing scale every 4-6 weeks. Blood was collected from the mouse tail after 4 hours of fasting (from 9 am to 1 pm) every 4-6 weeks using paraoxon-coated capillaries, and plasma was obtained through centrifugation.

In *APOE*3-Leiden.CETP* mice, the weight of organs/tissues, including liver, gonadal white adipose tissue (gWAT), subcutaneous white adipose tissue (sWAT), interscapular brown adipose tissue (iBAT), subscapular brown adipose tissue (sBAT), spleen, kidneys heart and adrenals were measured at the end of the experiment. Plasma levels of TC, TG and PL were measured using enzymatic kits (Roche Diagnostics, Germany). Lipoprotein profiles were determined from pooled plasma samples collected at week 16 (equal plasma volumes per mouse of each group) by fast protein liquid chromatography (FPLC) with a Superose 6 column (Cytiva, USA), followed by measurement of PL, TG and TC levels in the obtained fractions by enzymatic kits (Roche Diagnostics, Germany). Plasma HDL-C and HDL-PL levels were measured in the supernatant after precipitating ApoB-containing lipoproteins as previously described,[16] using the enzymatic kit for TC and PL (Roche Diagnostics, Germany).



In *Ldlr*$^{-/-}$ mice, the plasma levels of TC, TG, PL and HDL-C were measured using colorimetric assays (TC&TG: SOBIODA, France; PL: Phospholipids FS, DiaSys; HDL-C: HDL-C direct FS, DiaSys). Non-HDL-C levels were calculated by subtracting HDL-C from TC.

Plasma TC exposure was determined by calculating the area under the curve of plasma TC levels over the experimental period.

**In vivo organ/tissue uptake of VLDL-like particles and LDL**

In *APOE*3-Leiden.CETP* mice, at 17 weeks after virus injection, subgroups of mice (n=8) with body weight and plasma lipids close to the group mean were intravenously injected with glycerol tri[$^{3}$H]oleate ([$^{3}$H]TO) and [$^{14}$C]cholesteryl oleate ([$^{14}$C]CO) double-labeled very low-density lipoprotein (VLDL)-like particles (1.0 mg TG in 200 µL saline per mouse) or [$^{3}$H]TO and [$^{14}$C]CO double-labeled human LDL (0.2 mg TC in 200 µL saline per mouse) as described before.[12] Mice were killed by $CO_2$ inhalation at 15 min after injection of VLDL-like particles or at 30 min after injection of LDL and perfused with ice-cold PBS before organs/tissues were collected. Samples were dissolved overnight at 55°C in Solvable (PerkinElmer, The Netherlands) and then were mixed with Ultima Gold liquid scintillation cocktail (PerkinElmer, The Netherlands). $^{3}$H and $^{14}$C activity in the samples (disintegrations per min) were measured using a Tri-Carb 2910TR low-activity liquid scintillation analyzer

(PerkinElmer, The Netherlands). The uptake of $^{3}H$ and $^{14}C$ radioactivity by the organs/tissues was expressed as the percentage of injected radioactive dose.

**Fecal cholesterol and fecal bile acid quantification**

In *APOE*3-Leiden.CETP* mice, at 10 weeks after virus injection, feces were collected during 48 hours to determine lipid excretion. After freeze-drying, fecal samples were homogenized in 90% isopropanol at 0.05 mg/µL. To 5 µL of this homogenate, 10 µL 400 µg/mL cholesterol-d7 (Avanti, USA) in ethanol (Merck, USA), 10 µL water (Honeywell Riedel-de Haën, Germany) and 65 µL ethanol was added. Subsequently, samples were hydrolyzed at 70°C for 1 hour by adding 10 µL 10 M sodium hydroxide (Sigma Aldrich, USA). Cholesterol was extracted on a Strata™-X 33 µm Polymeric Reverse Phase solid phase 1 mL extraction tube (Phenomenex, USA). The cartridge was activated with methanol (Merck, USA), and equilibrated with water, after which the sample was loaded. Thereafter, samples were washed with water, eluted using methyl formate (Sigma Aldrich, USA) and the combined organic extract was dried. Cholesterol was derivatized by adding 50 µL N-methyl-N-trimethylsilyltrifluoroacetamide containing 1% trimethylchlorosilane (Thermo Fisher Scientific, USA) and 10% N-trimethylsilyl-imidazole (Thermo Fisher Scientific, USA). Finally, 150 µL tert-butyl methyl ether (Sigma Aldrich, USA) was added. Samples were analyzed on a gas chromatograph (8890 GC system; Agilent, USA) coupled to a mass spectrometer (5977B GC/MSD; Agilent, USA) equipped with an electron ionization source. Samples (1 µL) were injected splitless at 300°C. Cholesterol was separated on a VF-5ms column (Agilent, USA), and helium was used as carrier gas at a flow of 1 mL/min. The oven was set as follows: 1 min at 175°C, increase to 290°C at 50°C/min, increase to 310°C at 5°C/min, 5.7 min at 310°C. The transfer line was set at 280°C, the source at 230°C and the quadrupole at 150°C. For cholesterol-d7 *m/z* 336.4 (quantifier), 375.4, 465.5 and for cholesterol *m/z* 459.4 (quantifier), 354.3, 444.4 were used. Cholesterol was quantified using an external calibration line.

Bile acids in feces were analyzed as described elsewhere[17] with minor modifications. Dried feces were homogenized in 75% MeOH (4 mg/mL) and the homogenate was centrifuged at 18,213 g for 5 min at 20°C. The supernatant was taken, 4 µL, and spiked with 20 µL internal standard solution (500 ng/mL) and further diluted by the addition of 90 µL MeOH and 90 µL water. The samples were measured using a Shimadzu Nexera LC40 system, consisting of a DGU-405 degasser, two LC-40D X3 pumps, a SIL-40C X3 autosampler and a CTO-40S column oven (Shimadzu, USA). The gradient used was as follows: 0 to 0.2 min, constant at 20% B; 0.2 to 0.5 min, linear increase to 49% B; 0.5 to 5.5 min, linear increase to 64% B; 5.5 to 7.9 min, linear increase to 100% B; 7.9 to 9.9 min, constant at 100% B.

**Liver histology and lipid content**

In *APOE*3-Leiden.CETP* mice, liver samples were collected and fixated with phosphate-buffered formaldehyde and embedded in paraffin and cross-sectioned (5 µm thickness).

Sections were stained with hematoxylin-eosin (HE) and the lipid area was quantified using ImageJ software v1.52a. Hepatic lipids were extracted from snap-frozen liver samples according to a modified method from Bligh and Dyer.[18] Hepatic TG and TC levels were measured using enzymatic kits (Roche Diagnostics, Germany). Hepatic protein concentrations were measured using a BCA Protein assay kit (Thermo Fisher Scientific, USA). Hepatic lipid levels were expressed as nmol per mg protein.

**Gene expression analysis**

Total RNA was isolated from snap-frozen liver, sWAT, or aorta samples with TriPure RNA Isolation Reagent (Sigma Aldrich, USA) and the concentration of isolated RNA was determined by Nanodrop technology (Thermo Fisher Scientific, USA). Then, 1 µg RNA of each sample was reverse-transcribed into cDNA using Moloney murine leukemia virus reverse transcriptase (Promega, USA). Quantitative real-time PCR was performed using the GoTaq Real-Time PCR Detection Master Mix (Promega, USA) on a CFX386 machine (Bio-Rad, USA) according to the manufacturer's protocol. The expression of mRNA level was normalized to Beta-actin (*Actb*) and glyceraldehyde-3-phosphate dehydrogenase (*Gapdh*) mRNA expression and expressed as fold change compared with the eGFP or WT-LIPC group using the 2 to the power of -ΔΔCt method. The primer sequences are listed in Supplemental Table S1.



**Atherosclerosis visualization and quantification**

At 17 weeks after virus injection into *APOE*3-Leiden.CETP* mice, mice were killed by $CO_2$ inhalation followed by heart puncture and then perfused with ice-cold PBS. Hearts were collected, fixed in phosphate-buffered formaldehyde, and then embedded in paraffin. After cross-sectioning (5 µm thickness) throughout the aortic root area, 4 consecutive sections per heart at 50 µm intervals (starting at the opening of the aortic valves) were treated with hematoxylin phloxine saffron (HPS) to stain macrophages/nuclei/cellular components (hematoxylin; blue-purple), smooth muscle cells/cytoplasm (phloxine; pink-red), and collagen/fibrous caps (saffron; yellow) within atherosclerotic lesions. According to the guidelines of the American Heart Association adapted for mice,[19,20] lesions were categorized into mild lesions (type I-III) or severe lesions (type IV-V). Smooth muscle cells were stained using an anti-α-actin antibody (1:1000 dilution; Dako, Denmark) and a secondary antibody EnVision System-Horseradish peroxidase Labeled Polymer (1:400 dilution; Dako, Denmark) that was visualized by Liquid DAB + Substrate Chromogen System (Dako, Denmark). Collagen was stained with Sirius Red (Sigma Aldrich, USA). Macrophages were stained with an anti-Mac-3 antibody (1:1000 dilution; BD Pharmingen, USA), a Horseradish peroxidase-labeled secondary antibody and a peroxide substrate (1:400 dilution; Vector Laboratories, USA). Stained slides were scanned with a 3DHistech Pannoramic 250 Flash III DX (3DHistech, Hungary). Lesion areas and the areas of smooth muscle cells, collagen and macrophages

were quantified using ImageJ software v1.52a. The lesion stability index was calculated as the ratio of stable markers (i.e. smooth muscle cell area and collagen area) per unstable marker (i.e. macrophage area).

At 14 weeks after virus injection, *Ldlr*$^{-/-}$ mice were anesthetized with i.p. injection of a mixture of ketamine (100 mg/kg) and xylazine (20 mg/kg) followed by heart puncture and then perfused with ice-cold PBS. The aortic arches, with the major arteries that stem from them (brachiocephalic, left common carotid and left subclavian), were dissected under a microscope, frozen in optimal cutting temperature medium (O.C.T.; Sakura, USA) and stored at -80°C before serial cryo-sectioning. The aortic roots were dissected under a microscope and frozen in O.C.T. medium and stored at -80°C before serial cryo-sectioning and oil red O staining. Cryostat sections were cut at -20°C using a CryoStar NX70 cryostat (Thermo Fisher Scientific, USA). Sections of 5 µm thickness were harvested (when the three arteries were visible of the aortic arches; when the three aortic valve leaflets were visible of the aortic roots), mounted on SuperFrost Plus glass slides (Thermo Fisher Scientific, USA) and stored at -80°C until use as described.[21] Oil red O (Sigma Aldrich, USA) was used to stain neutral lipids according to the protocol of Mehlem, et al.[22] Stained slides were scanned with a Hamamatsu C9600-12 NanoZoomer HT Scanner (Hamamatsu, Japan) within 24 hours. The lesion area was quantified using NDP.view2 software (Hamamatsu, Japan).



**Statistical analysis**

Data were analyzed by GraphPad Prism Software v9.3.1. A one-way ANOVA with a Tukey correction for multiple comparisons was used for comparing the effects of treatments. Data are shown as mean ± SEM. $P < 0.05$ was considered significant.

## Results

**HL-E97G improves dyslipidemia in *APOE*3-Leiden.CETP* mice fed with a Western-type diet**

Female *APOE*3-Leiden.CETP* mice were fed a Western-type diet were injected intravenously with AAV8-TGB-*eGFP* (control), AAV8-TGB-*LIPC* (HL-WT), or AAV8-TGB-*LIPC* E97G (HL-E97G) (**Figure 1A**). HL-E97G and HL-WT, but not control virus injection, resulted in expression of human *LIPC* (*hLIPC*) in the liver (**Figure 1B**), but not in other extrahepatic tissues such as sWAT (**Figure S1A**) and aorta (**Figure S1B**). The expression of HL-E97G and HL-WT did not affect hepatic expression of endogenous mouse *Lipc* (*mLipc*; **Figure 1C)**. HL-E97G and HL-WT did not affect body weight (**Figure 1D**) and the weight of organs/tissues (**Figure 1E**). In line with its specifically enhanced phospholipase activity (**Figure S1C**&**D**)[12] HL-E97G induced a profound and sustained reduction in plasma PL compared to the control group (-40% vs control; -22% vs HL-WT at week 16; **Figure 1F**) and an increased lysophospholipid/

phospholipid ratio, while HL-WT was marginally effective (-24% vs control; **Figure 1F**). Likewise, HL-E97G induced a profound reduction in plasma TG (-44% vs control; -31% vs HL-WT; **Figure 1G**) and TC (-48% vs control; -30% vs HL-WT; **Figure 1H**), while HL-WT was much less effective. FPLC profiling of pooled plasma showed that HL-E97G mainly reduced PL, TG and TC within (V)LDL fractions (**Figure 1I**-**K**). In fact, the decrease in TC by HL-E97G was explained by a major decrease in non-HDL-C (-50% vs control; -32% vs HL-WT; **Figure 1L**) and a milder decrease in HDL-C (-24% vs control; **Figure 1M**) without changing the gross composition of HDL (i.e. cholesterol and phospholipid; **Figure S1E&F**). HL-E97G largely decreased TC exposure (i.e. the area under the curve of cholesterol during 16 weeks) versus both control (-63%) and HL-WT (-58%) (**Figure 1N**).

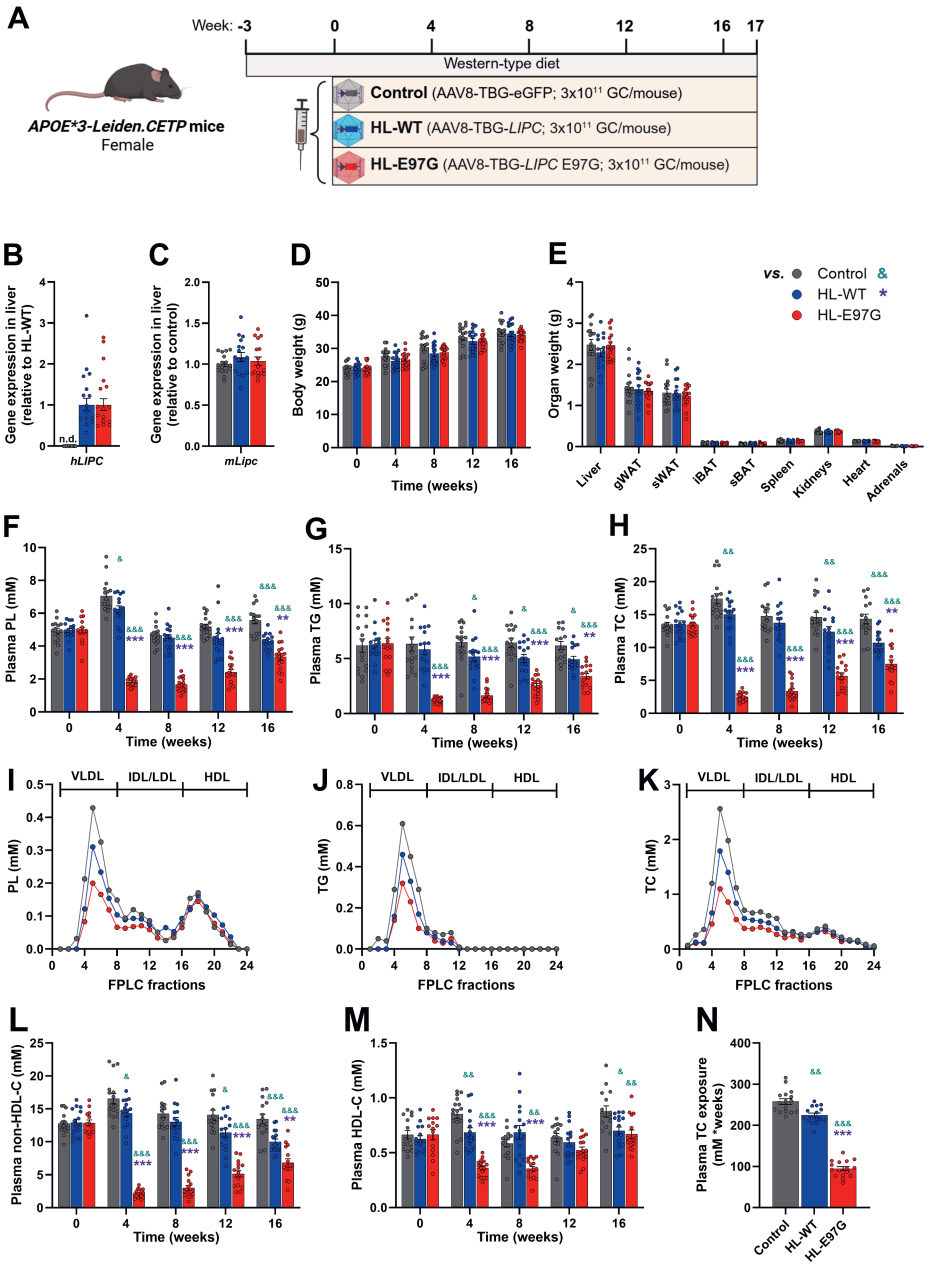


**Figure 1. Human HL-E97G expression reduces plasma phospholipid, triglyceride and cholesterol levels in *APOE*3.Leiden.CETP* mice.** *APOE*3.Leiden.CETP* mice fed a Western-type diet received an intravenous injection with $3\times10^{11}$ genome copies (GC) of adeno-associated viruses (AAV8) expressing either enhanced green fluorescent protein (eGFP; control), the human *LIPC* gene encoding wildtype HL (HL-WT), or the human *LIPC* gene encoding the gain-of-function E97G variant of HL (HL-E97G). Throughout the experimental period, 4-hour fasted blood samples were collected to obtain plasma (at week 0, 4, 8, 12 and 16) and mice were killed after 17 weeks of virus injection and organs/tissues were

collected (**A**). Hepatic expression of human HL (*hLIPC*; **B**) and mouse HL (*mLipc;* **C**) were determined. Body weight (**D**) and organ weight (**E**) were recorded. Plasma levels of phospholipids (PL; **F**), triglycerides (TG; **G**), and total cholesterol (TC; **H**) were determined. In pooled plasma samples collected at week 16, lipoproteins were separated by fast protein liquid chromatography (FPLC) to measure PL (**I**), TG (**J**) and TC (**K**) levels in collected fractions. Plasma non-high-density lipoprotein cholesterol (non-HDL-C; **L**) and HDL-C (**M**) levels were measured. Plasma TC exposure (**N**) was calculated from TC levels throughout the experimental period. Data are shown as mean ± SEM (B-H and L-N, n = 14-16/group). Differences were assessed using one-way ANOVA with a Tukey correction for multiple comparisons. $^{\&}$ $P < 0.05$, $^{\&\&}$ $P < 0.01$, $^{\&\&\&}$ $P < 0.001$, compared with the control group. ** $P < 0.01$, *** $P < 0.001$, compared with the HL-WT group. gWAT, gonadal white adipose tissue; HL, hepatic lipase; *hLIPC*, human hepatic lipase; iBAT, interscapular brown adipose tissue; *mLipc*, mouse hepatic lipase; sBAT, subscapular brown adipose tissue; sWAT, subcutaneous white adipose tissue.

### HL-E97G increases V(LDL) uptake by liver in *APOE*3-Leiden.CETP* mice

To directly evaluate the effect of HL-E97G on lipoprotein kinetics, we intravenously injected *APOE*3-Leiden.CETP* mice with either VLDL-like particles (**Figure 2A**-**D**) or human LDL (**Figure 2E**-**H**) that were labeled with [$^{3}$H]TO and [$^{14}$C]CO. For both VLDL-like particles and LDL, HL-E97G increased the uptake of [$^{3}$H]TO and [$^{14}$C]CO by the liver, while HL-WT did not (**Figure 2A, C, E and G**). HL-E97G also slightly increased the uptake of [$^{3}$H]TO and [$^{14}$C]CO from LDL by spleen, heart, sBAT and adrenals (**Figure 2B**, **D**, **F** and **H**). These data suggest that HL-E97G reduces plasma lipids in part by increasing (V)LDL uptake by the liver, with a plausible additional contribution from extrahepatic tissues.

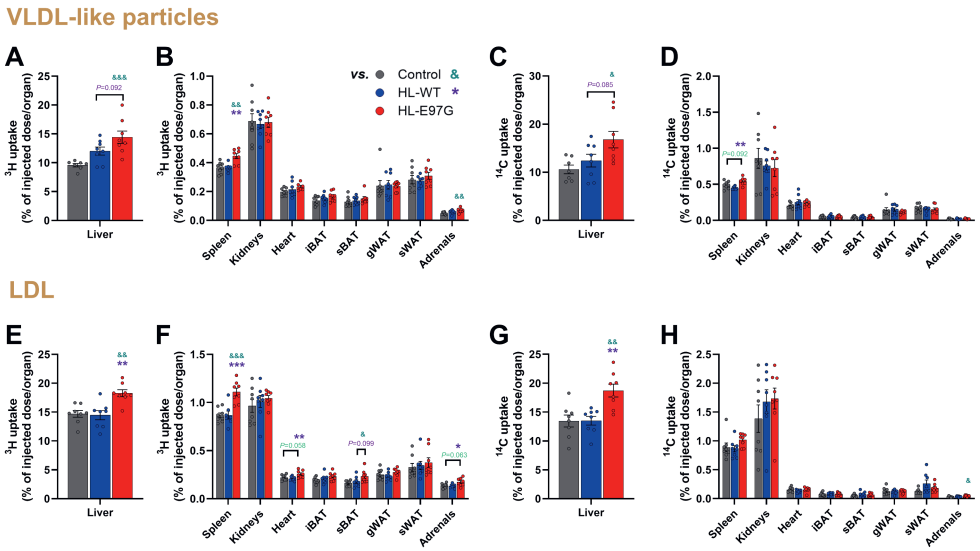


**Figure 2. Human HL-E97G expression increases uptake of V(LDL) uptake by the liver and extrahepatic tissues in *APOE*3-Leiden.CETP* mice.** *APOE*3.Leiden.CETP* mice, after 17 weeks of virus injection, were intravenously injected with glycerol tri[$^{3}$H]oleate ([$^{3}$H]TO) and [$^{14}$C]cholesteryl oleate ([$^{14}$C]CO) double-labeled very low-density lipoprotein (VLDL)-like particles or LDL. At 15 min after injection of VLDL-like particles, mice were killed and organs/tissues were collected. The activity of $^{3}$H and $^{14}$C in the liver (**A**, **C**) and other organs/tissues (**B**, **D**) were measured. At 30 min after injection of LDL, the activity of $^{3}$H and $^{14}$C in the liver (**E**, **G**) and other organs/tissues (**F**, **H**) were measured. Data are shown as mean ± SEM (n = 6-8/group). Differences were assessed using one-way ANOVA with a Tukey correction for multiple comparisons. $^{\&}$ $P < 0.05$, $^{\&\&}$ $P < 0.01$, $^{\&\&\&}$ $P < 0.001$, compared with the control group. * $P < 0.05$, ** $P < 0.01$, *** $P < 0.001$, compared with the HL-WT group. gWAT, gonadal white adipose tissue; iBAT, interscapular brown adipose tissue; sBAT, subscapular brown adipose tissue; sWAT, subcutaneous white adipose tissue.

### HL-E97G does not affect hepatic lipid content and fecal lipid excretion in *APOE*3-Leiden.CETP* mice

Since HL-E97G increased (V)LDL uptake by the liver, we next investigated the impact on liver lipids. HL-E97G and WL-WT did not affect liver histology (**Figure 3A**), hepatic lipid area (**Figure 3B**), or hepatic contents of TG (**Figure 3C**), TC (**Figure 3D**) and PL (**Figure 3E**). Likewise, HL-E97G did not affect excretion of feces (**Figure 3F**), fecal cholesterol (**Figure 3G**) and fecal bile acids contents (**Figure 3H**), suggesting that HL-E97G does not affect lipid excretion. Also, HL-E97G did not alter the hepatic expression of genes involved in lipogenesis, cholesterol synthesis or VLDL production (**Figure 3I**), suggesting that HL-E97G does not affect VLDL production. While HL-E97G increased (V)LDL uptake by the liver, hepatic expression of *Pcsk9 and Ldlr* were not affected (**Figure 3J**). Collectively, these data indicate that HL-E97G does not induce liver steatosis and toxicity.

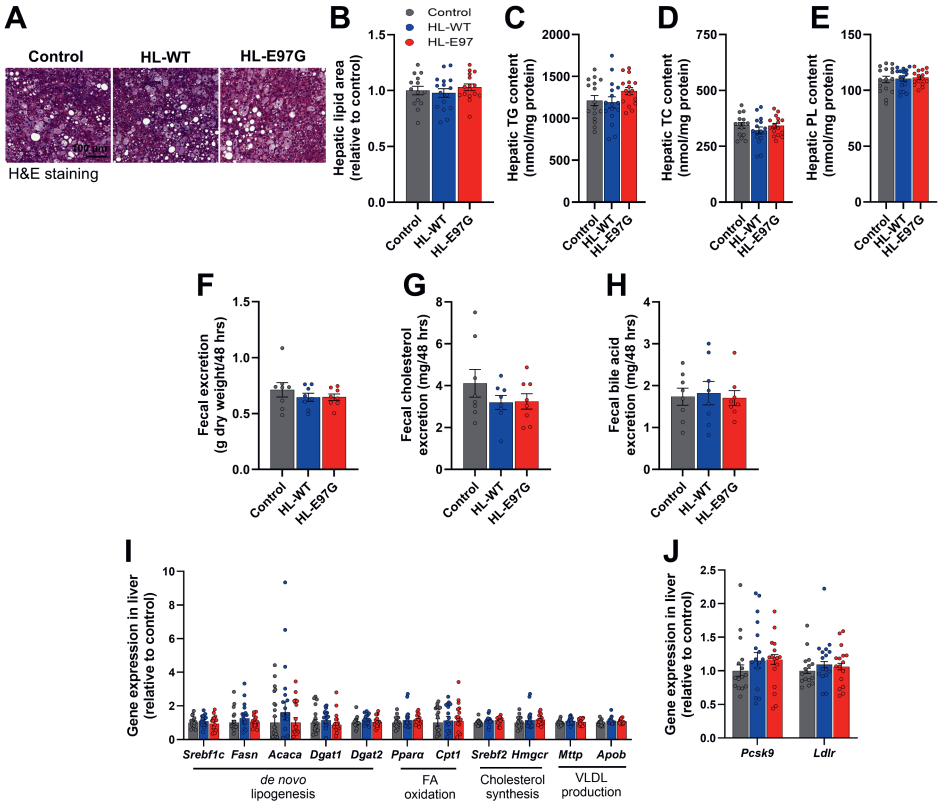


**Figure 3. HL-E97G expression does not affect hepatic lipid content and fecal lipid excretion in *APOE*3-Leiden.CETP* mice.** At 17 weeks after virus injection into *APOE*3.Leiden.CETP mice*, liver samples were collected and stained with hematoxylin-eosin (H&E; **A**) and the hepatic lipid area (**B**) was quantified. Hepatic triglyceride (TG; **C**), total cholesterol (TC; **D**) and phospholipid (PL; **E**) contents were determined. After 10 weeks of virus injection, feces were collected for 48 hours and fecal excretion (**F**), fecal cholesterol (**G**) and bile acid (**H**) excretion were measured. The expression of genes involved in *de novo* lipogenesis synthesis, fatty acid (FA) oxidation, cholesterol synthesis and very low-density lipoprotein (VLDL) production (**I**) and genes involved in lipoprotein uptake (**J**) was determined in the liver. Data are shown as mean ± SEM (**B**-**E**, **I** and **J**, n = 14-16/group; **F**-**H**, n = 8/group). Differences were assessed using one-way ANOVA with a Tukey correction for multiple comparisons. *Acc1*, acetyl coenzyme A carboxylase 1; *Apob*, apolipoprotein B; *Cpt1*, carnitine palmitoyl transferase 1; *Dgat1*, diacylglycerol O-acyltransferase 1; *Dgat2*, diacylglycerol O-acyltransferase 2; *Fasn*, fatty acid synthase; *Hmgcr*, 3-hydroxy-3-methylglutaryl coenzyme A; *Ldlr*, low density lipoprotein receptor; *Mttp*, microsomal triglyceride transfer protein; *Pcsk9*, proprotein convertase subtilisin/kexin type 9; *Ppara*, peroxisome proliferator-activated receptor alpha; *Srebf1c*, sterol regulatory element-binding factor 1c; *Srebf2*, sterol regulatory element-binding factor 2.

**HL-E97G decreases atherosclerotic lesion area and severity in *APOE*3-Leiden.CETP* mice**

Since HL-E97G largely reduced plasma TC, the most important risk factor for atherosclerosis, we next determined the atherosclerotic lesion size in the aortic root at 17 weeks after virus injection. Representative examples of HPS-stained sections are shown in **Figure 4A**. HL-E97G profoundly decreased the atherosclerotic lesion size throughout the aortic root (**Figure 4B**), resulting in a significant reduction of the average lesion size (-98% vs control; -97% vs HL-WT; **Figure 4C**) while HL-WT did not significantly affect lesion size (**Figure 4B**&**C**). Further characterization of lesions revealed that HL-E97G largely increased the percentage of unaffected sections (4-fold vs control; 5-fold vs HL-WT; **Figure 4D**), with 7/16 mice devoid of lesions. In fact, the lesions that were present in the HL-E97G expressing mice were all mild, compared with 35% severe lesions in controls and HL-WT expressing mice (**Figure 4E**). Next, the composition of lesions was determined (i.e. smooth muscle cell and collagen as stability markers of lesions; macrophage as instability marker of lesions) (**Figure 4F**) to reveal that although HL-E97G did not grossly affect lesion composition (**Figure 4G**), it improved the lesion stability index (i.e. sum of smooth muscle cell and collagen area divided by macrophage area) of type III lesions (**Figure 4H**). Taken together, our data show that HL-E97G but not HL-WT markedly attenuates atherosclerotic lesion development in *APOE*3.Leiden.CETP* mice.



**>> Figure 4. Human HL-E97G expression reduces atherosclerotic area and severity in *APOE*3.Leiden.CETP* mice.** At 17 weeks after virus injection into *APOE*3.Leiden.CETP mice*, aortic root samples were collected and stained with hematoxylin phloxine saffron (HPS; **A**). The atherosclerotic lesion areas of 4 consecutive sections (with 50 µm intervals) were quantified and plotted as a function of the distance from open aortic valves (**B**). Average atherosclerotic lesion areas (**C**) were calculated from **B**. The undiseased areas were recorded and normalized to total areas (**D**). Lesions were categorized according to lesion severity, expressed as a percentage of total lesions (**E**), and shown by lesion severity: mild (type I-III, on the left) and severe (type IV-V, on the right). Representative cross-sections of aortic root labeled with anti-α-smooth muscle cell actin (α-actin), Sirius red and anti-MAC3 antibody (MAC3) were shown (**F**). The smooth muscle cell, collagen and macrophage areas (**G**) were quantified in type III lesions and the lesion stability index (i.e. the sum of the smooth muscle cell and collagen area divided by macrophage area) of type III lesions (**H**) was measured. Data are shown as mean ± SEM (**B-D,** n = 14-16/group; **E, G** and **H**, n = 16 in control or HL-WT group n = 9 or 7 in HL-E97G group because 7 or 9 mice did not have lesions at all or type III lesions, respectively). Differences were assessed using one-way ANOVA with a Tukey correction for multiple comparisons. **&&** $P < 0.01$, **&&&** $P < 0.001$, compared with the control group. ****** $P < 0.01$, ******* $P < 0.001$, compared with the HL-WT group.

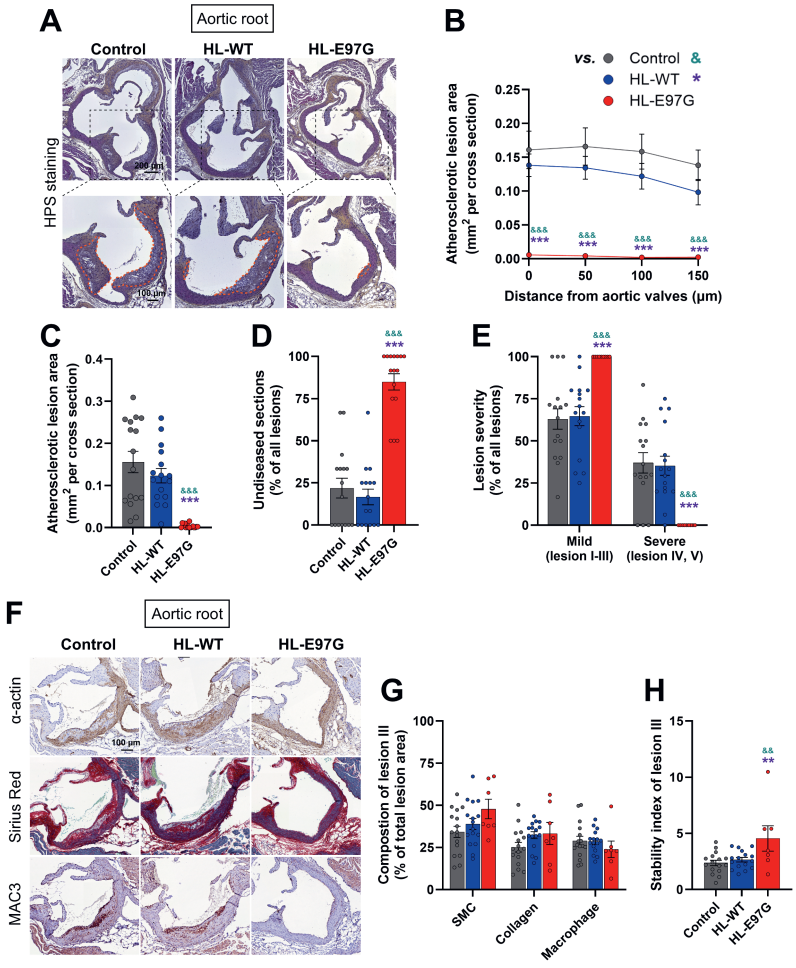


**HL-E97G improves dyslipidemia and reduces atherosclerosis in *Ldlr*$^{-/-}$ mice**

To assess whether the lipid-lowering effect of HL-E97G is dependent on the LDLR pathway, we next evaluated the effects of HL-E97G versus HL-WT on plasma lipids and atherosclerosis development in *Ldlr*$^{-/-}$ mice. To this end, male and female *Ldlr*$^{-/-}$ mice fed with a proatherogenic diet received an intravenous injection of AAV8-TGB-*eGFP* (control), AAV8-TGB-*LIPC* (HL-WT) or AAV8-TGB-*LIPC* E97G (HL-E97G) (**Figure 5A**). Similar to *APOE*3-Leiden.CETP* mice, HL-E97G did not affect body weight (**Figure 5B**) and markedly reduced plasma PL (-75% vs control; -68% vs HL-WT; **Figure 5C**), plasma TG (-89% vs control; -80% vs HL-WT; **Figure 5D**) and TC levels (-79% vs control; -77% vs HL-WT at week 14; **Figure 5E**) in *Ldlr*$^{-/-}$ mice. HL-E97G also decreased both non-HDL-C (-86% *vs* control; -83% vs HL-WT; **Figure 5F**) and HDL-C (-69% vs control; -66% vs HL-WT; **Figure 5G**) levels. Similar to *APOE*3-*

*Leiden.CETP* mice, HL-E97G markedly reduced plasma TC exposure (-80% vs control; -77% vs HL-WT) in *Ldlr*$^{-/-}$ mice (**Figure 5H**).

Next, we measured atherosclerotic lesion size in both the aortic root and aortic arch after 14 weeks of virus injection. Representative examples of oil Red O-stained sections are shown for the aortic root (**Figure 5I**) and aortic arch (**Figure 5K**). While HL-WT did not reduce or worsen aortic atherosclerotic lesions compared to the control group in the aortic root (**Figure 5J**) or arch (**Figure 5L**), HL-E97G reduced the lesion area in the aortic root lesions (-54% vs control; -41% vs HL-WT; **Figure 5J**) and even more strongly in the aortic arch (-73% vs control; -71% vs HL-WT; **Figure 5L**). Although small group sizes precluded statistical analysis in males and females separately, HL-E97G seemed to consistently reduce plasma lipids and atherosclerotic lesion area in both sexes (**Figure S2A-I**).

These data demonstrate for the first time that HL-E97G reduced plasma lipids independent of the LDLR pathway and can effectively delay and reduce the progression of atherosclerosis in mice lacking LDLR.



**>> Figure 5. Human HL-E97G expression improves dyslipidemia and decreases atherosclerotic lesion area in *Ldlr*$^{-/-}$ mice.** *Ldlr*$^{-/-}$ mice fed with a pro-atherogenic diet received an intravenous injection with $3\times10^{11}$ genome copies (GC) of adeno-associated viruses (AAV8) expressing either enhanced green fluorescent protein (eGFP; control), the human *LIPC* gene encoding wildtype HL (HL-WT), or the human *LIPC* gene encoding the gain-of-function E97G variant of HL (HL-E97G). Throughout the experimental period, 3-hour fasted blood samples were collected to obtain plasma (at week 0, 4, 8, and 14). Mice were killed 14 weeks after virus injection, and the aortic root and arch were collected (**A**). Body weight (**B**) was recorded throughout the experimental period. Plasma phospholipid (PL; **C**) levels were measured at week 14. Plasma triglyceride (TG; **D**), and total cholesterol (TC; **E**) levels throughout the experimental period were determined. Plasma non-high-density lipoprotein cholesterol (non-HDL-C; **F**) and HDL-C (**G**) levels were measured at week 14. Plasma TC exposure (**H**) was calculated from TC levels throughout the experimental period. Representative cross-sections of the aortic root (**I**) and sagittal section of aortic arch (**K**) stained with oil red O are shown, and atherosclerotic lesion areas were quantified (**J** and **L**). Data are shown as mean ± SEM (n = 7-10/group). Differences were assessed using one-way ANOVA with a Tukey correction for multiple comparisons. **&** $P < 0.05$, **&&&** $P < 0.001$, compared with the control group. ***** $P < 0.05$, ****** $P < 0.01$, ******* $P < 0.001$, compared with the HL-WT group. HL, hepatic lipase.

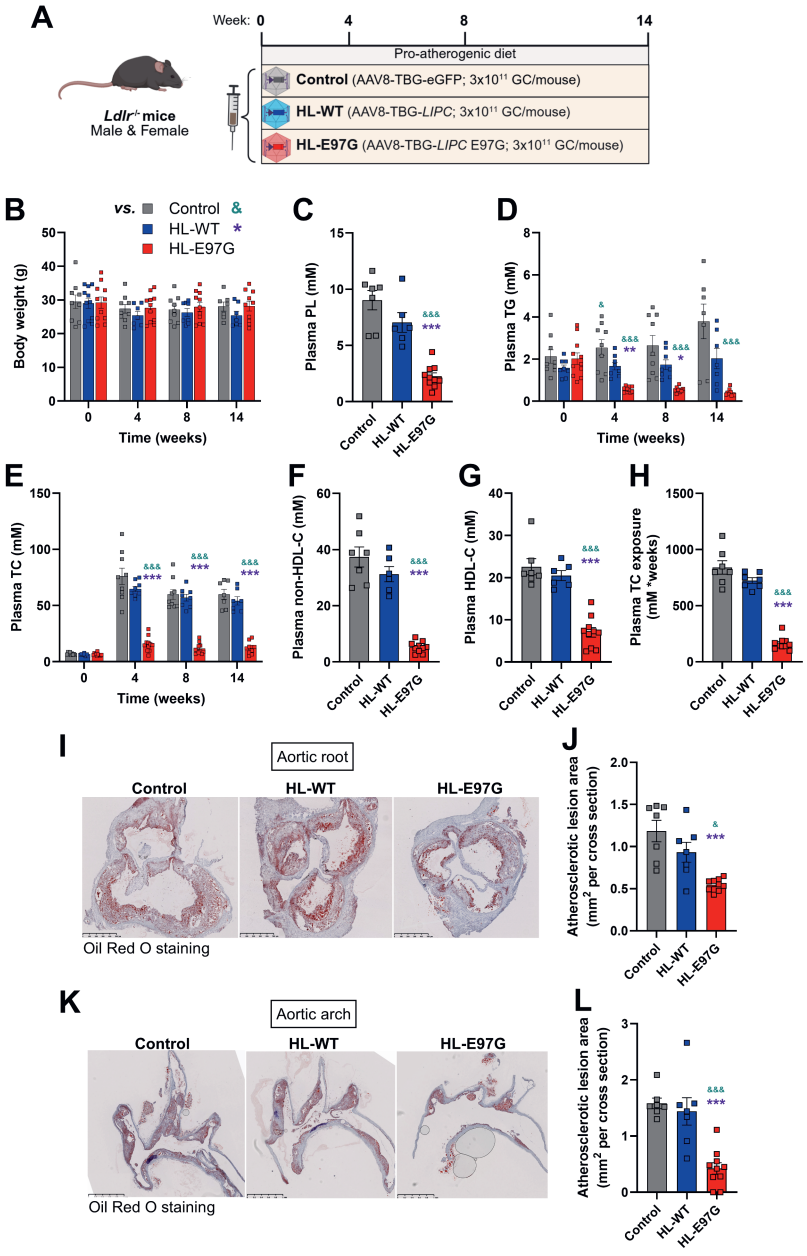
A
Week: 0
4
8
14
Pro-atherogenic diet
Control (AAV8-TBG-eGFP; 3x10¹¹ GC/mouse)
HL-WT (AAV8-TBG-LIPC; 3x10¹¹ GC/mouse)
HL-E97G (AAV8-TBG-LIPC E97G; 3x10¹¹ GC/mouse)
Ldlr-/- mice
Male & Female
B
vs. Control &
HL-WT *
HL-E97G
Body weight (g)
Time (weeks)
C
Plasma PL (mM)
D
Plasma TG (mM)
Time (weeks)
E
Plasma TC (mM)
Time (weeks)
F
Plasma non-HDL-C (mM)
G
Plasma HDL-C (mM)
H
Plasma TC exposure (mM*weeks)
Control
HL-WT
HL-E97G
I
Aortic root
Control
HL-WT
HL-E97G
Oil Red O staining
J
Atherosclerotic lesion area (mm² per cross section)
K
Aortic arch
Control
HL-WT
HL-E97G
Oil Red O staining
L
Atherosclerotic lesion area (mm² per cross section)

## Discussion

The HL-E97G variant leading to a specific increase in HL phospholipase activity was recently identified in a family with combined hypocholesterolemia phenotype characterized by a fall in both plasma LDL-C and HDL-C concentrations.[12] The functional characterization performed in this study has allowed us to extend our knowledge of this variant. We have shown for the first time that HL-E97G not only lowers cholesterol levels, in part through increased hepatic uptake of (V)LDL, but also significantly prevents atherosclerotic lesions, in contrast to the wild-type form of HL. We also demonstrate that HL-E97G exerts its cholesterol-lowering action independently of LDLR and that it is also able of protecting *Ldlr*$^{-/-}$ mice from atherosclerosis. These data validate the extreme therapeutic interest of HL-E97G for the treatment of hypercholesterolemia, particularly the most severe forms such as HoFH.



The role of HL in the development of atherosclerosis remains a subject of debate. On the one hand, HL lowers HDL-C and increases small dense LDL concentrations, both of which can contribute to atherosclerosis.[23,24] On the other hand, HL can also exert anti-atherogenic properties by promoting the clearance of lipoprotein remnants and potentially the reverse cholesterol transport by increasing b-HDL levels.[25-27] In *Ldlr*$^{-/-}$ mice, the genetic deletion of HL promotes the premature development of atherosclerotic plaques.[28] Conversely, transgenic re-expression of HL in either *Ldlr*$^{-/-}$ or apolipoprotein E knockout mice significantly reduces atherosclerotic plaque development, and this effect is dependent on the enzymatic functions of HL.[26,28] Genetic data have failed to clarify the role of HL, with again discordant results according to study populations. Individuals with complete HL deficiency are very rare and some of these individuals did develop ASCVD whereas other did not.[13,25,29] However, low HL activity was associated with an increased risk of coronary heart diseases.[30] In accordance with this observation, a Mendelian randomization study demonstrated that low HL activity was causally related to higher ASCVD risk,[31] but this has not been confirmed in other similar studies using the same genetic variant.[32,33] Thus, while there is a tendency towards a negative association between HL activity and ASCVD risk, this effect is modest and not always consistent. In the present study, expression of the wild-type form of HL had indeed a much more modest effect on total cholesterol exposure than the HL-E97G variant, and this did not translate into a reduction in atherosclerotic lesions. These data confirm the unique value of the HL-E97G variant for its specific modulation of HL activity.

Regarding the mechanism of action of the HL-E97G variant, we have previously shown that it specifically increases the phospholipase activity of HL, to the detriment of its TG lipase activity, possibly linked to a change in the conformational structure of the lid domain.[12] We observed that HL-E97E lowered HDL-C, without altering its overall composition. Although HDL-C is inversely correlated with ASCVD in humans, Mendelian Randomization studies did

not provide evidence for a causal role of HDL-C in ASCVD,[34] and raising HDL-C by CETP inhibition has been futile with respect to affecting ASCVD outcomes.[35] Thus, the reduction of HDL-C by HL-E97G observed in our models is not expected to affect atherosclerosis.

To go further, we performed kinetic experiments using VLDL-like particles and purified human LDL, and we observed that HL-E97G overexpression moderately increases (V)LDL particles hepatic uptake, without substantially affecting peripheral tissues uptake, such as the adipose tissue or the heart. In our previous study, we also performed kinetic experiments on *APOE*3.Leiden.CETP* mice with VLDL-like particles and murine VLDL, and the particles hepatic uptake was not increased in mice overexpressing HL-E97G. Instead, particles uptake was significantly increased in adipose tissue (both white and brown) and oxidative tissues such as the heart or the muscle in the HL-E97G group.[12] On the other hand, this study confirms previous data[12] showing that HL-E97G does not affect either faecal cholesterol or bile acid excretion in APOE*3.Leiden.CETP mice. This apparent discrepancy between our two studies and between the increase in hepatic uptake of (V)LDL and the lack of effect on faecal cholesterol excretion is surprising and still unexplained. Further research is therefore needed to understand in detail the molecular mechanisms underlying the cholesterol-lowering effect of HL-E97G. However, these kinetic experiments in both studies indicate that no significant differences in the tissue clearance profile were observed between the VLDL-like particles (without apoB) and endogenous murine VLDL[12] or human LDL (with apoB) confirming that HL-E97G did not act through an apoB-mediated pathway.

The present results are also encouraging with regard to the positioning of HL-E97G as a new therapeutic target for the management of hypercholesterolemia. Indeed, it was crucial to verify its effect on the development of atherosclerosis, given that the proband in whom this variant was identified has developed coronary artery disease.[12] It remains unclear however whether such ASCVD was due to altered HL activity or other CV risk factors (the proband had type 2 diabetes and a history of heavy smoking). It is also important to mention that to date none of the other familial carriers of HL-E97G have reported similar cardiovascular events. The therapeutic benefit of this new cholesterol-lowering mechanism of action mediated by HL-E97G is that it is independent of the action of LDLR, unlike statins or PCSK9 inhibitors. This suggests that it may act synergistically with these classes of LLTs. Above all, it offers future prospects for the therapeutic management of patients with HoFH associated with bi-allelic variants without LDLR activity (“null” alleles). In this group of patients, current therapies are based on LDL-apheresis, evinacumab[36] or lomitapide.[37] The use of lomitapide is limited by the development of liver steatosis, which requires regular liver monitoring, and by significant gastrointestinal disorders, which necessitate the introduction of a long-term low-fat diet.[38] Evinacumab, a monoclonal antibody that inhibits the action of ANGPTL3, also acts via an LDLR-independent pathway. In a randomized controlled trial, it has been shown to decrease plasma LDL-C levels of around 50% in HoFH patients, independently of residual LDLR activity.[39] Interestingly, recent studies suggested that the LDL-C reduction induced by

ANGPTL3 inhibition is associated with an increased EL activity and subsequent accelerated LDL catabolism.[40,41] Since HL-E97G variant has a lipase activity closer to that of EL, with predominantly phospholipase activity, this underlines the importance of this enzymatic activity in regulating circulating lipoprotein concentrations. It would therefore be important to determine whether HL-E97G and evinacumab act via common pathways.

In conclusion, this study confirms the potential therapeutic interest of the HL-E97G variant, which is characterized by an increase in HL phospholipase activity, a reduction in circulating lipoproteins without inducing hepatic lipid accumulation and, above all, protection against the development of atherosclerosis in two different mouse models. Its mechanism of action is still under investigation, but implies both a hepatic and extra-hepatic pathway, independent of LDLR, to promote lipoprotein catabolism. Together, this study advances our understanding of lipoprotein metabolism and opens up interesting therapeutic perspectives for HoFH patients lacking functional LDLR.



## Data availability

The data underlying this article will be shared on reasonable request to the corresponding authors.

## Funding

This work was supported by the French national research project CHOPIN (CHolesterol Personalized INnovation) funded by the Agence Nationale de la Recherche (ANR-16-RHUS-0007) and coordinated by the CHU of Nantes; the INSTINCTIVE research program funded by the Fondation pour la Recherche Médicale (FRM: EQU201903007846); The HEPALIPA project funded by the Agence Nationale de la Recherche (ANR-R23121NN/RPV23156NNA), the Chinese Scholarship Council (grant 202006850007 to XG) and the Netherlands Cardiovascular Research Initiative: an initiative with support of the Dutch Heart Foundation (CVON-GENIUS-2), and the Dutch Heart Foundation (Established Investigator grant 2009T038 to PCNR).

## Acknowledgement

The authors would like to express their gratitude to Dr Thibaut Quillard, from the Vascular and Pulmonary Diseases team, for his sound and useful advice on the analysis of atherosclerosis in mice. Graphics were created with BioRender.com.

## Authors' contributions

TS and XG designed the study, carried out the research, analyzed and interpreted the results, and wrote and revised the manuscript. XG was responsible for designing, executing, and analyzing all experiments with the *APOE*3-Leiden.CETP* mouse model (Figures 1, 2, 3 and 4; Supplemental Figure 1). MS, AT, SF PL, VL, LK, ACMP, RL TCMS, SA, WD, SS, MH, NB, MG, MDF, PM advised the study, carried out the research, analyzed, interpreted the results, and reviewed the manuscript. SK, BC, PCNR and CLM designed and advised the study, interpreted the results, edited, reviewed and revised the manuscript and obtained funding.



## Conflict of Interest

None declared.

## References


1. Roth G. A., Mensah G. A., Johnson C. O., et al. Global Burden of Cardiovascular Diseases and Risk Factors, 1990-2019: Update From the GBD 2019 Study. J. Am. Coll. Cardiol. 76, 2982–3021 (2020).
2. Vaduganathan M., Mensah G. A., Turco J. V., et al. The Global Burden of Cardiovascular Diseases and Risk: A Compass for Future Health. J. Am. Coll. Cardiol. 80, 2361–2371 (2022).
3. Borén J., Chapman M. J., Krauss R. M., et al. Low-density lipoproteins cause atherosclerotic cardiovascular disease: pathophysiological, genetic, and therapeutic insights: a consensus statement from the European Atherosclerosis Society Consensus Panel. Eur. Heart J. 41, 2313–2330 (2020).
4. Zhang Y., Pletcher M. J., Vittinghoff E., et al. Association Between Cumulative Low-Density Lipoprotein Cholesterol Exposure During Young Adulthood and Middle Age and Risk of Cardiovascular Events. JAMA Cardiol 6, 1406–1413 (2021).
5. Mach F., Baigent C., Catapano A. L., et al. 2019 ESC/EAS Guidelines for the management of dyslipidaemias: lipid modification to reduce cardiovascular risk. Eur. Heart J. 41, 111–188 (2020).
6. Ray K. K., Molemans B., Schoonen W. M., et al. EU-Wide Cross-Sectional Observational Study of Lipid-Modifying Therapy Use in Secondary and Primary Care: the DA VINCI study. Eur J Prev Cardiol 28, 1279–1289 (2021).
7. Ray K. K., Haq I., Bilitou A., et al. Treatment gaps in the implementation of LDL cholesterol control among high- and very high-risk patients in Europe between 2020 and 2021: the multinational observational SANTORINI study. Lancet Reg Health Eur 29, 100624 (2023).
8. Tromp T. R., Hartgers M. L., Hovingh G. K., et al. Worldwide experience of homozygous familial hypercholesterolaemia: retrospective cohort study. Lancet 399, 719–728 (2022).
9. Raal F. J., Hegele R. A., Ruzza A., et al. Evolocumab Treatment in Pediatric Patients With Homozygous Familial Hypercholesterolemia: Pooled Data From Three Open-Label Studies. Arterioscler. Thromb. Vasc. Biol. 44, 1156–1164 (2024).
10. Gu J., Gupta R. N., Cheng H. K., et al. Current treatments for the management of homozygous familial hypercholesterolaemia: a systematic review and commentary. Eur J Prev Cardiol 31, 1833–1849 (2024).
11. Raal F. J., Rosenson R. S., Reeskamp L. F., et al. Evinacumab for Homozygous Familial Hypercholesterolemia. N. Engl. J. Med. 383, 711–720 (2020).
12. Dijk W., Di Filippo M., Kooijman S., et al. Identification of a Gain-of-Function LIPC Variant as a Novel Cause of Familial Combined Hypocholesterolemia. Circulation 146, 724–739 (2022).
13. Santamarina-Fojo S., González-Navarro H., Freeman L., et al. Hepatic lipase, lipoprotein metabolism, and atherogenesis. Arterioscler. Thromb. Vasc. Biol. 24, 1750–1754 (2004).
14. van Vlijmen B. J., van 't Hof H. B., Mol M. J., et al. Modulation of very low density lipoprotein production and clearance contributes to age- and gender- dependent hyperlipoproteinemia in apolipoprotein E3-Leiden transgenic mice. J. Clin. Invest. 97, 1184–1192 (1996).
15. van Eenige R., Verhave P. S., Koemans P. J., et al. RandoMice, a novel, user-friendly randomization tool in animal research. PLoS One 15, e0237096 (2020).
16. In Het Panhuis W., Kooijman S., Brouwers B., et al. Mild Exercise Does Not Prevent Atherosclerosis in APOE*3-Leiden.CETP Mice or Improve Lipoprotein Profile of Men with Obesity. Obesity (Silver Spring) 28 Suppl 1, S93–s103 (2020).
17. van Eenige R., Ying Z., Tambyrajah L., et al. Cannabinoid type 1 receptor inverse agonism attenuates dyslipidemia and atherosclerosis in APOE∗3-Leiden.CETP mice. J. Lipid Res. 62, 100070 (2021).

18. Bligh E. G., Dyer W. J. A rapid method of total lipid extraction and purification. Can. J. Biochem. Physiol. 37, 911–917 (1959).
19. Wong M. C., van Diepen J. A., Hu L., et al. Hepatocyte-specific IKKβ expression aggravates atherosclerosis development in APOE*3-Leiden mice. Atherosclerosis 220, 362–368 (2012).
20. van der Vaart J. I., van Eenige R., Rensen P. C. N., et al. Atherosclerosis: an overview of mouse models and a detailed methodology to quantify lesions in the aortic root. Vasc. Biol. 6, e230017 (2024).
21. Bessueille L., Kawtharany L., Quillard T., et al. Inhibition of alkaline phosphatase impairs dyslipidemia and protects mice from atherosclerosis. Transl. Res. 251, 2–13 (2023).
22. Mehlem A., Hagberg C. E., Muhl L., et al. Imaging of neutral lipids by oil red O for analyzing the metabolic status in health and disease. Nat. Protoc. 8, 1149–1154 (2013).
23. Jansen H., Verhoeven A. J., Sijbrands E. J. Hepatic lipase: a pro- or anti-atherogenic protein? J. Lipid Res. 43, 1352–1362 (2002).
24. Zambon A., Deeb S. S., Hokanson J. E., et al. Common variants in the promoter of the hepatic lipase gene are associated with lower levels of hepatic lipase activity, buoyant LDL, and higher HDL2 cholesterol. Arterioscler. Thromb. Vasc. Biol. 18, 1723–1729 (1998).
25. Connelly P. W., Hegele R. A. Hepatic lipase deficiency. Crit. Rev. Clin. Lab. Sci. 35, 547–572 (1998).
26. Dichek H. L., Brecht W., Fan J., et al. Overexpression of hepatic lipase in transgenic mice decreases apolipoprotein B-containing and high density lipoproteins. Evidence that hepatic lipase acts as a ligand for lipoprotein uptake. J. Biol. Chem. 273, 1896–1903 (1998).
27. Dichek H. L., Johnson S. M., Akeefe H., et al. Hepatic lipase overexpression lowers remnant and LDL levels by a noncatalytic mechanism in LDL receptor-deficient mice. J. Lipid Res. 42, 201–210 (2001).
28. Freeman L., Amar M. J., Shamburek R., et al. Lipolytic and ligand-binding functions of hepatic lipase protect against atherosclerosis in LDL receptor-deficient mice. J. Lipid Res. 48, 104–113 (2007).
29. Knudsen P., Antikainen M., Uusi-Oukari M., et al. Heterozygous hepatic lipase deficiency, due to two missense mutations R186H and L334F, in the HL gene. Atherosclerosis 128, 165–174 (1997).
30. Dugi K. A., Brandauer K., Schmidt N., et al. Low hepatic lipase activity is a novel risk factor for coronary artery disease. Circulation 104, 3057–3062 (2001).
31. Silbernagel G., Scharnagl H., Kleber M. E., et al. LDL triglycerides, hepatic lipase activity, and coronary artery disease: An epidemiologic and Mendelian randomization study. Atherosclerosis 282, 37–44 (2019).
32. Johannsen T. H., Kamstrup P. R., Andersen R. V., et al. Hepatic lipase, genetically elevated high-density lipoprotein, and risk of ischemic cardiovascular disease. J. Clin. Endocrinol. Metab. 94, 1264–1273 (2009).
33. Fan Y. M., Raitakari O. T., Kähönen M., et al. Hepatic lipase promoter C-480T polymorphism is associated with serum lipids levels, but not subclinical atherosclerosis: the Cardiovascular Risk in Young Finns Study. Clin. Genet. 76, 46–53 (2009).
34. Voight B. F., Peloso G. M., Orho-Melander M., et al. Plasma HDL cholesterol and risk of myocardial infarction: a mendelian randomisation study. Lancet 380, 572–580 (2012).
35. Lincoff A. M., Nicholls S. J., Riesmeyer J. S., et al. Evacetrapib and Cardiovascular Outcomes in High-Risk Vascular Disease. N. Engl. J. Med. 376, 1933–1942 (2017).
36. Béliard S., Saheb S., Litzler-Renault S., et al. Evinacumab and Cardiovascular Outcome in Patients With Homozygous Familial Hypercholesterolemia. Arterioscler. Thromb. Vasc. Biol. 44, 1447–1454 (2024).

37. Cuchel M., Raal F. J., Hegele R. A., et al. 2023 Update on European Atherosclerosis Society Consensus Statement on Homozygous Familial Hypercholesterolaemia: new treatments and clinical guidance. Eur. Heart J. 44, 2277–2291 (2023).
38. Ben-Omran T., Masana L., Kolovou G., et al. Real-World Outcomes with Lomitapide Use in Paediatric Patients with Homozygous Familial Hypercholesterolaemia. Adv. Ther. 36, 1786–1811 (2019).
39. Raal F. J., Rosenson R. S., Reeskamp L. F., et al. The Long-Term Efficacy and Safety of Evinacumab in Patients With Homozygous Familial Hypercholesterolemia. JACC Adv 2, 100648 (2023).
40. Adam R. C., Mintah I. J., Alexa-Braun C. A., et al. Angiopoietin-like protein 3 governs LDL-cholesterol levels through endothelial lipase-dependent VLDL clearance. J. Lipid Res. 61, 1271–1286 (2020).
41. Wu L., Soundarapandian M. M., Castoreno A. B., et al. LDL-Cholesterol Reduction by ANGPTL3 Inhibition in Mice Is Dependent on Endothelial Lipase. Circ. Res. 127, 1112–1114 (2020).

# Supplemental Materials

## Supplemental Table & Figures

**Table S1. Primer sequences for quantitative real-time PCR**

| | Primers | |
|---|---|---|
| Gene | Forward (5'- 3') | Reverse (5'- 3') |
| *Acc1* | AACGTGCAATCCGATTTGTT | GAGCAGTTCTGGGAGTTTCG |
| *Actb* | AACCGTGAAAAGATGACCCAGAT | CACAGCCTGGATGGCTACGTA |
| *Apob* | GCCCATTGTGGACAAGTTGATC | CCAGGACTTGGAGGTCTTGGA |
| *Cpt1* | GAGACTTCCAACGCATGACA | ATGGGTTGGGGTGATGTAGA |
| *Dgat1* | TCCGTCCAGGGTGGTAGTG | TGAACAAAGAATCTTGCAGACGA |
| *Dgta2* | TCGCGAGTACCTGATGTCTG | CTTCAGGGTGACTGCGTTCT |
| *Fasn* | GCGCTCCTCGCTTGTCGTCT | TAGAGCCCAGCCTTCCATCTCCTG |
| *Gapdh* | GGGGCTGGCATTGCTCTCAA | TTGCTCAGTGTCCTTGCTGGGG |
| *Hmgcr* | CCGGCAACAACAAGATCTGTG | ATGTACAGGATGGCGATGCA |
| *hLIPC* | GGCTGGAGGAATCTGTGCAA | AGAAAGACGATTGCTGGGGG |
| *Ldlr* | GCATCAGCTTGGACAAGGTGT | GGGAACAGCCACCATTGTTG |
| *mLipc* | GTCGCTGCTGGGAACAAAAF | GGATCAACTCGCCGATGTCT |
| *Mttp* | CTCTTGGCAGTGCTTTTTCTCT | GAGCTTGTATAGCCGCTCATT |
| *Pcsk9* | TGTGAGGTCCCACTCTGTG | GCTTCTGCTCCAGAGGTCA |
| *Ppara* | ATGCCAGTACTGCCGTTTTC | GGCCTTGACCTTGTTCATGT |
| *Srebf1c* | AGCCGTGGTGAGAAGCGCAC | ACACCAGGTCCTTCAGTGATTTGCT |
| *Srebf2* | TGAAGCTGGCCAATCAGAAAA | ACATCACTGTCCACCAGACTGC |

*Acc1*, acetyl coenzyme A carboxylase 1; *Actb*, beta-actin; *Apob*, apolipoprotein B; *Cpt1*, carnitine palmitoyl transferase 1; *Dgat1*, diacylglycerol O-acyltransferase 1; *Dgat2*, diacylglycerol O-acyltransferase 2; *Fasn*, fatty acid synthase; *Gapdh*, glyceraldehyde-3-phosphate dehydrogenase; *Hmgcr*, 3-hydroxy-3-methylglutaryl coenzyme A; *hLIPC*, human hepatic lipase; *Ldlr*, low density lipoprotein receptor; *mLipc*, mouse hepatic lipase; *Mttp*, microsomal triglyceride transfer protein; *Pcsk9*, proprotein convertase subtilisin/kexin type 9; *Ppara*, peroxisome proliferator-activated receptor alpha; *Srebf1c*, sterol regulatory element-binding factor 1c; *Srebf2*, sterol regulatory element-binding factor 2.

**Supplemental Figure S1. Human HL-E97G expression increases the ratio of lysophospholipids/ phospholipids in *APOE*3.Leiden.CETP* mice.**

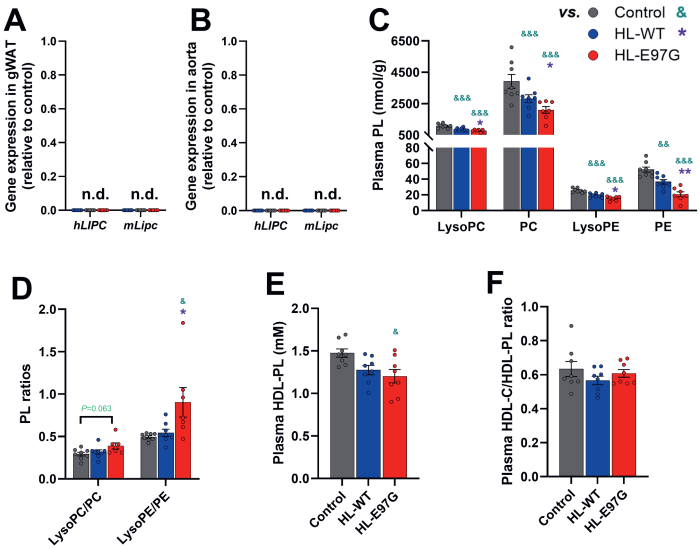


At 17 weeks after virus injection into *APOE*3.Leiden.CETP* mice, gWAT and aorta samples were collected and the expression of human *LIPC* (*hLIPC*) and endogenous mouse *Lipc* (*mLipc*) was measured in gWAT (**A**) and aorta (**B**). At week 16, plasma levels of the phospholipids (PL) lysophosphatidylcholine (LysoPC), phosphatidylcholine (PC), lysophosphatidylethanolamine (LysoPE) and (phosphatidylethanolamine (PE) were measured (**C**). The ratios of LysoPC/PC and LysoPE/PE were determined (**D**). At week 16, plasma levels of high-density lipoprotein phospholipid (HDL-PL) were measured (**E**) and the ratio of plasma HDL-cholesterol (HDL-C, Figure 1M)/HDL-PL was determined (**F**). Data are shown as mean ± SEM (n = 7-8/group). Differences were assessed using one-way ANOVA with a Tukey correction for multiple comparisons. $^{\&}$ $P < 0.05$, $^{\&\&}$ $P < 0.01$, $^{\&\&\&}$ $P < 0.001$, compared with the control group. * $P < 0.05$, ** $P < 0.01$, compared with the HL-WT group.

**Supplemental Figure S2. Human HL-E97G expression improves dyslipidemia and decreases atherosclerotic lesion area in both male and female *Ldlr*$^{-/-}$ mice.**

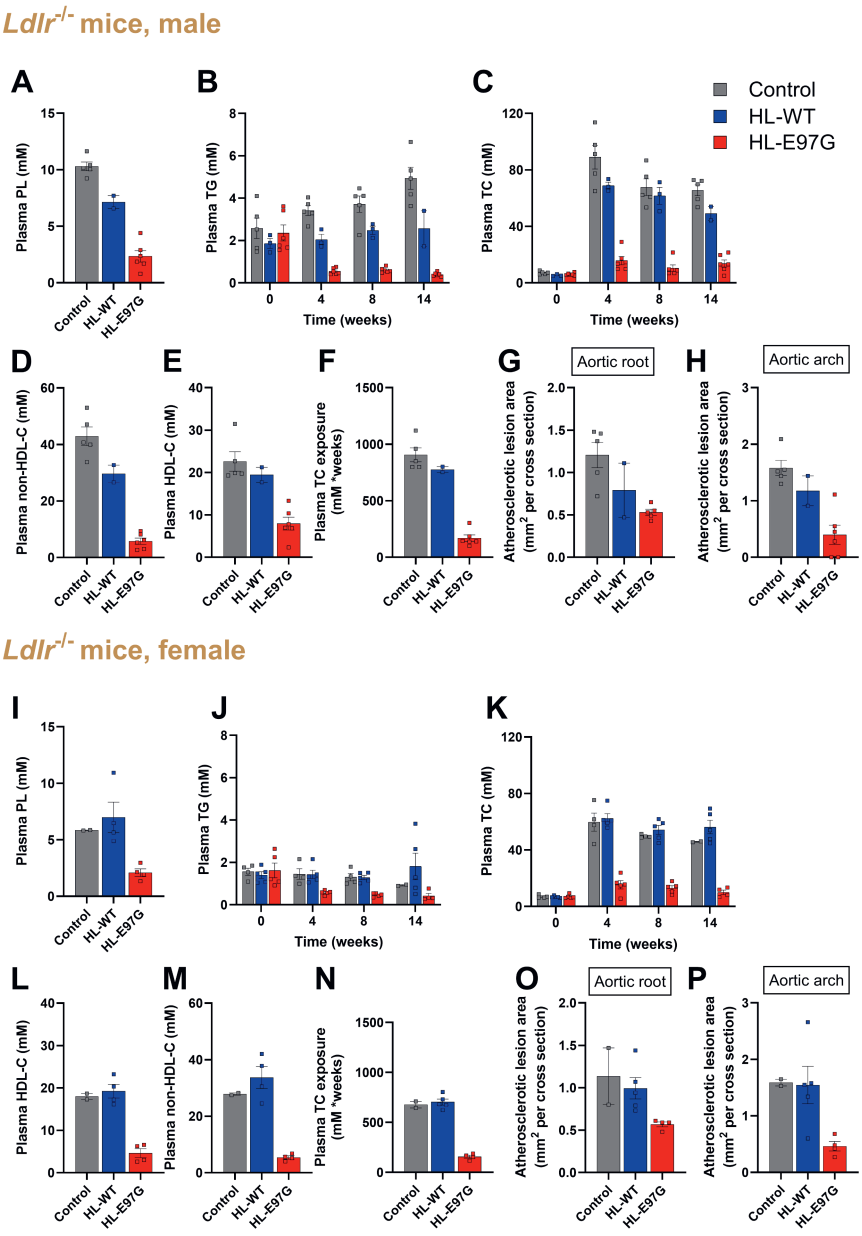


This figure represents the distribution of **Figure 5** data by sex of mice. 14 weeks after virus injection into *Ldlr*$^{-/-}$ mice, plasma phospholipid (PL, **A/I**) levels were measured. Plasma total cholesterol (TC) and triglycerides (TG) were measured in both males (**B**, **C**) and females (**J**, **K**) throughout the experimental procedure. Plasma high-density lipoprotein cholesterol (HDL-C, **E/L**) and non-HDL-C

(**D**/**M**) levels were measured. Plasma TC exposure level was calculated throughout the experimental period **(F**/**N**)**.** The atherosclerotic lesion areas of aortic roots (**G**/**0**) and sagittal section of aortic arches were quantified (**H**/**P**). Data are shown as mean ± SEM (n = 2-6/group).

## Expanded Materials & Methods

**Plasma phospholipid composition quantification**

In *APOE*3-Leiden.CETP* mice, 4 hours of fasting plasma samples were obtained after 16 weeks of virus injection. To 15 µL of plasma, 150 µL MeOH, 25 µL internal standard solution and 600 µL MTBE was added, and vortexed. Samples were left at room temperature for 30 min, and were centrifuged at 18.213 g for 5 min at 20°C. 650 µL of supernatant was taken and transferred to a new 2 mL Eppendorf tube. This extraction was then repeated with the original samples by adding both 300 µL of MTBE and 100 µL of MeOH. All samples were vortexed and centrifuged at 18.213 g for 15 min at 20°C. 400 µL of the supernatant was transferred to the Eppendorf tubes containing the previous 650 µL of supernatant. To these tubes, 300 µL of water was added and the samples were centrifuged at 18.213 g for 5 min at 20°C. From the upper organic layer, 650 µL of supernatant was transferred to a 1.5 mL glass vial. This supernatant was dried at room temperature under a gentle stream of nitrogen. The dried samples were reconstituted in 300 µL running buffer (50: 50 MeOH: DCM with 10 mM ammonium acetate) and then were transferred to a glass insert before injecting to a mass spectrometer (QTRAP 5500; AB Sciex, USA). Samples were analyzed on the expanded Lipidyzer platform. The detailed procedure has been described elsewhere.[1,2]



## Supplemental references

1. Ghorasaini M., Mohammed Y., Adamski J., et al. Cross-Laboratory Standardization of Preclinical Lipidomics Using Differential Mobility Spectrometry and Multiple Reaction Monitoring. Anal. Chem. 93, 16369–16378 (2021).
2. Su B., Bettcher L. F., Hsieh W. Y., et al. A DMS shotgun lipidomics workflow application to facilitate high-throughput, comprehensive lipidomics. J. Am. Soc. Mass Spectrom. 32, 2655–2663 (2021).